Trigger and offline selection of $\mathrm{B}^0_\mathrm{S} \to \mathrm{J}/\psi(\mathrm{ee})\phi$

Note

Issue:	1
Revision:	1
Reference:	LHCb-2008-079
Created:	[redacted]
Last modified:	September, 2009

Prepared by: Adlène Hicheur [a]
EPFL, Switzerland

LHCb-2008-079
11/09/2009

[a] Adlene.Hicheur@cern.ch

Document Status Sheet

1. Document Title: Trigger and offline selection of $\mathrm{B_s^0} \to \mathrm{J/\psi(ee)\phi}$			
2. Document Reference Number: LHCb-2008-079			
3. Issue	**4. Revision**	**5. Date**	**6. Reason for change**
Draft	1	July, 2009	First draft

Contents

1 Introduction

$\mathrm{B_s^0} \to \mathrm{J/\psi(\mu\mu)\phi(KK)}$ is considered as the "golden" channel for the extraction of the CP violating phase caused by the interference between $\mathrm{B_s^0}$ mixing and decay. Beside the theoretical "cleanness" of $\mathrm{B_s^0} \to \mathrm{J/\psi\phi}$, the decay chain $\mathrm{B_s^0} \to \mathrm{J/\psi(\mu\mu)\phi(KK)}$ benefits from high trigger efficiency and very good reconstruction performances [1].
Although extraction of $2\beta_s$ with first data will focus on $\mathrm{B_s^0} \to \mathrm{J/\psi(\mu\mu)\phi(KK)}$, it is expected that other modes will be used in a combined fit [2], to improve the sensitivity. Beside these modes, $\mathrm{B_s^0} \to \mathrm{J/\psi(ee)\phi}$ appears to be one of the most promising in terms of statistics and will certainly play a important role in improving the precision of the measurement.
In this document, we present a first attempt of trigger and offline selection for $\mathrm{B_s^0} \to \mathrm{J/\psi(ee)\phi}$. We estimate the selection efficiency, the background levels and the expected yields for a integrated luminosity of $2\ fb^{-1}$.

2 Samples

For this study, we used signal and background DC06 simulated events:

- 247k $\mathrm{B_s^0} \to \mathrm{J/\psi(ee)\phi}$ phys-lumi2 events (produced with Gauss v25r7, Boole v12r10, Brunel v30r14)
- 852k inclusive $\mathrm{b\bar{b}}$ phys-v2-lumi2 events (produced with Gauss v25r10, Boole v12r10, Brunel v30r17)
- 175.4k inclusive $\mathrm{b\bar{b}}$ stripped events, corresponding to $\sim$ 6.1 millions events (produced with Gauss v25r7, Boole v12r10, Brunel v30r17)
- 987.5k inclusive $X \to \mathrm{J/\psi(ee)}$ events, mostly dominated by prompt production (produced with Gauss v25r8, Boole v12r10, Brunel v30r14).
- 1119885 L0-stripped minimum bias events for rate computation (produced with Gauss v25r7, Boole v12r4, Brunel v30r17).

3 Offline selection

3.1 Tracks and particle ID

The tracks used for the kaons and electrons are long tracks, with measurements upstream (Velo, TT) as well as downstream (T stations).
For the kaons, RICH particle ID is required, to reduce the pions background, by requiring the log likelihood difference to be positive $\Delta LL(K-\pi) > 0$. Figure 1 shows the distribution of this quantity for true kaons and background.

For the electrons, Calorimetry ID is used as well as bremsstrahlung recovery. The recovery algorithm [3] relies on the extrapolation of the electron Velo segment to the ECAL and matching with a nearby cluster. The electron momentum is corrected by adding the energy of the (photon) cluster to the track energy. We require that $\Delta LL(e-\pi) > 0$. Figure 2 shows the distribution of $\Delta LL(e-\pi)$ for electron candidates.

3.2 Intermediate resonances

3.2.1 $\phi \to \mathrm{K^+K^-}$

Kaons selected as described in the previous section are used to form $\phi \to \mathrm{K^+K^-}$ candidates. The K^+K^- vertex χ^2 per degree of freedom (figure 3) is required to be less than 20, the transverse momentum (figure 4) must be greater than $1\ \mathrm{GeV}/c$ and the invariant mass of the pair must lie within the window $[1005, 1035]\ \mathrm{MeV}/c^2$ (figure 5).

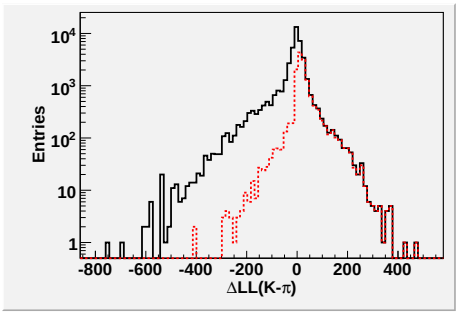

Figure 1 $\Delta LL(K-\pi)$ distribution for all kaons candidates (solid black line) and true kaons (red dashed line).

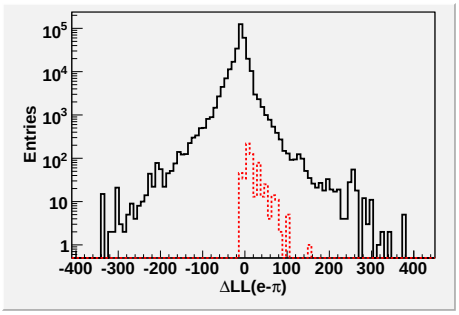

Figure 2 $\Delta LL(e-\pi)$ distribution for all electrons candidates (solid black line) and true electrons (red dashed line).

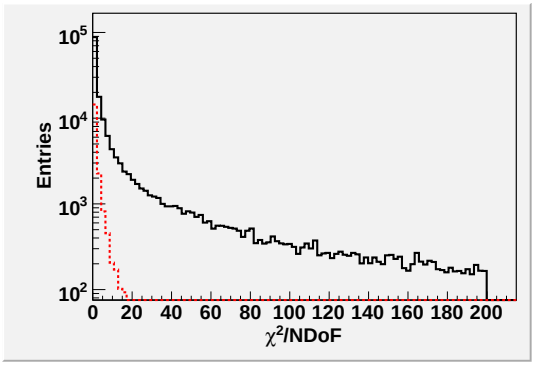

Figure 3 KK vertex $\chi^2/NDoF$ distribution for all KK pairs (solid black line) and true ϕ (red dashed line).

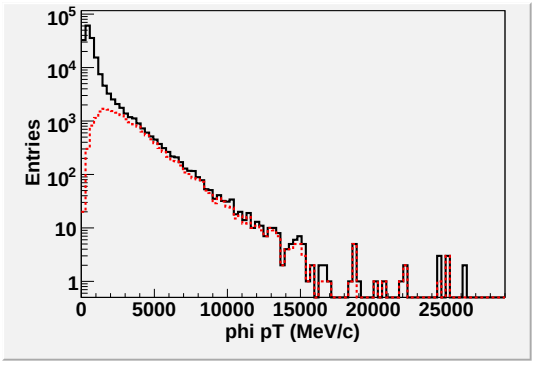

Figure 4 p_T distribution for ϕ candidates, all KK pairs (solid black line) and true ϕ (red dashed line).

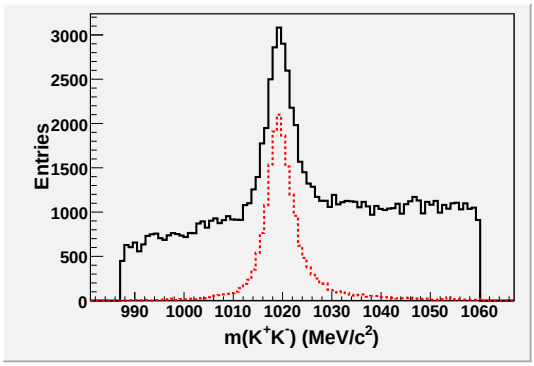

Figure 5 KK invariant mass distribution for all KK pairs (solid black line) and true ϕ (red dashed line). The distributions are obtained after applying kaon ID.

3.2.2 $\mathrm{J}/\psi \to \mathrm{e^+e^-}$

For the $\mathrm{J}/\psi \to \mathrm{e^+e^-}$ candidates, the e^+e^- vertex χ^2 per degree of freedom (figure 6) is required to be less than 20 and the invariant mass of the pair must lie within the window $[2700, 3300]$ MeV/c^2 (figure 7).

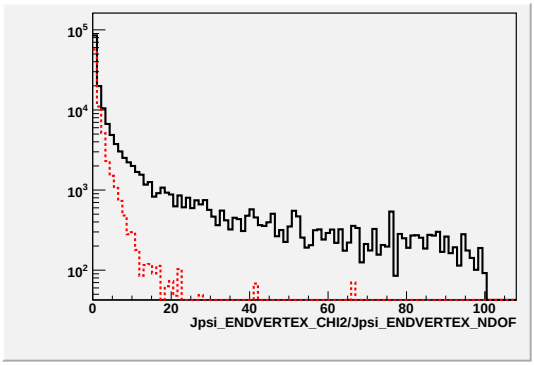

Figure 6 ee vertex $\chi^2/NDoF$ distribution for all ee pairs (solid black line) and true J/ψ (red dashed line).

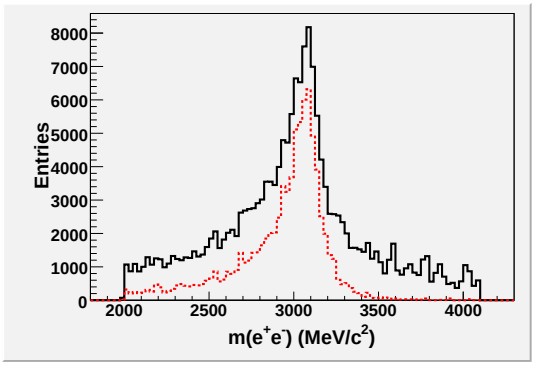

Figure 7 ee invariant mass distribution for all ee pairs (solid black line) and true J/ψ (red dashed line). The distributions are obtained after applying electron ID.

3.3 $\mathrm{B_s^0}$ candidates

$\mathrm{B_s^0}$ candidates are formed from $\phi \to \mathrm{K^+K^-}$ and $\mathrm{J}/\psi \to \mathrm{e^+e^-}$ combinations selected as described before. The following "geometrical" cuts are then applied:

- the cosine of the angle between the flight vector and the momentum (figure 8), $cos(\vec{F},\vec{p}) > 0.995$.
- the $\mathrm{B_s^0}$ impact parameter χ^2 (figure 9), $\chi^2_{IP}(\mathrm{B_s^0}) < 30$.
- the $\mathrm{B_s^0}$ vertex χ^2 per degree of freedom (figure 10), $\chi^2_{vtx}/NDoF < 60$.

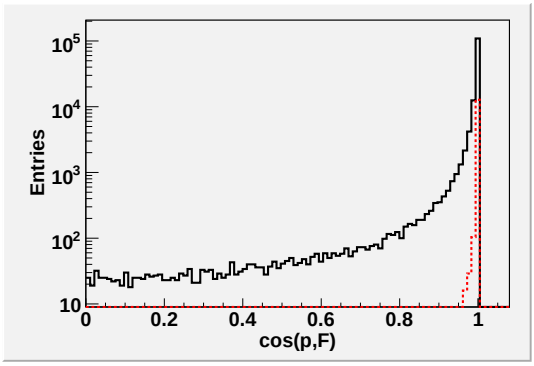

Figure 8 Cosine of the angle between the $\mathrm{B_s^0}$ flight vector and its momentum, for all candidates (solid black line) and true signal (red dashed line).

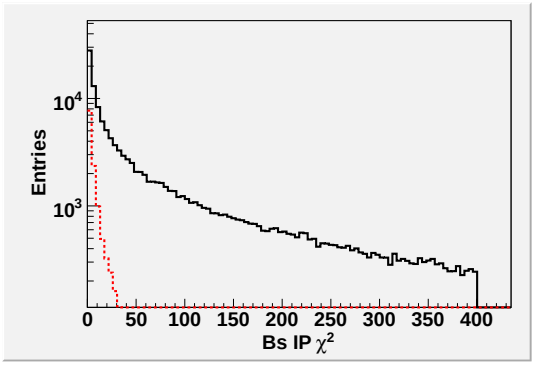

Figure 9 $\mathrm{B_s^0}$ IP χ^2 distribution for all candidates (solid black line) and true signal (red dashed line).

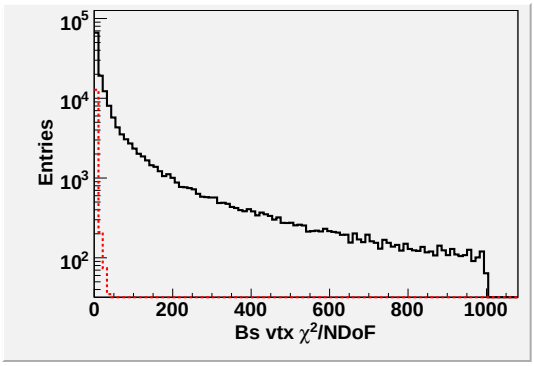

Figure 10 $\mathrm{B_s^0}$ vertex χ^2 per degree of freedom, distribution for all candidates (solid black line) and true signal (red dashed line).

Finally, we use the pseudo mass $m(\mathrm{B_s^0}) - m(\mathrm{J/\psi}) + m(\mathrm{J/\psi})^{PDG}$ instead of the reconstructed $\mathrm{B_s^0}$ mass as a discriminant variable (figure 11). The reason is that the pseudo mass resolution is much better than in the reconstructed mass case. The signal window is defined as $[5.2, 5.5]$ MeV/c^2 and the large window including the side bands is $[4.6, 6.2]$ MeV/c^2.

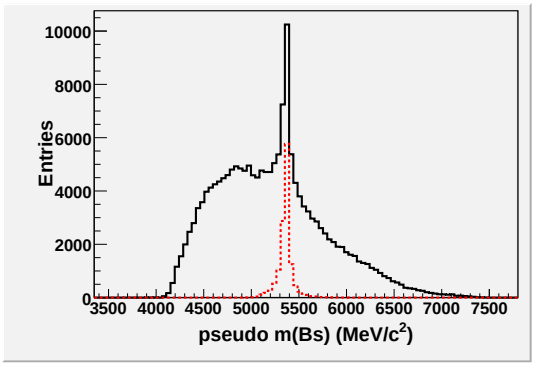

Figure 11 $\mathrm{B_s^0}$ pseudo mass, distribution for all candidates (solid black line) and true signal (red dashed line).

3.4 Summary of cuts and efficiencies

Table 1 summarizes the cuts effects on signal selection.

Cut	Efficiency [%]
$\mathrm{J/\psi(ee)}$ selection	
reconstructed	45.64 ± 0.10
e minimum $\Delta \ln \mathcal{L}_{\mathrm{e}\pi} > 0$	93.61 ± 0.10
e minimum $p_{\mathrm{T}} > 750\,\mathrm{MeV}/c$	88.08 ± 0.10
e minimum IPS > 1	89.35 ± 0.10
$\mathrm{J/\psi}$ $\chi^2_{\mathrm{vtx}}/\mathrm{nDoF} < 20$	100
$2700 < M(ee) < 3300$ MeV/c^2	77.44 ± 0.15
Total $\mathrm{J/\psi(ee)}$ selection	57.12 ± 0.12
$\phi \to \mathrm{K^+K^-}$ selection	
reconstructed	86.08 ± 0.08
K minimum $\Delta \ln \mathcal{L}_{\mathrm{K}\pi} > 0$	75.68 ± 0.09
ϕ $\chi^2_{\mathrm{vtx}}/\mathrm{nDoF} < 20$	100
$p_{\mathrm{T}}(\phi) > 1\,\mathrm{GeV}/c$	94.08 ± 0.10
$1005 < M(\mathrm{KK}) < 1035$ MeV/c^2	95.48 ± 0.10
Total $\phi \to \mathrm{K^+K^-}$ selection	67.99 ± 0.10
$\mathrm{B_s^0} \to \mathrm{J/\psi(ee)\phi}$ selection	
reconstructed	15.91 ± 0.07
$\mathrm{B_s^0}$ $\chi^2_{\mathrm{vtx}}/\mathrm{nDoF} < 60$	100
IP χ^2 $(\mathrm{B_s^0}) < 30$	94.42 ± 0.12
$\mathrm{B_s^0}$ pointing angle $cos(p, F) > 0.995$	98.65 ± 0.13
Pseudo $\mathrm{B_s^0}$ mass $5.2 < M < 5.5$ GeV/c^2	91.71 ± 0.18
Total $\mathrm{B_s^0}$ selection	85.43 ± 0.18
$\varepsilon_{\mathrm{cut}}$	42.06 ± 0.25
$\varepsilon_{\mathrm{L0}}/\varepsilon_{\mathrm{cut}}$	34.65 ± 0.37
$\varepsilon_{\mathrm{cut}} \times \varepsilon_{\mathrm{L0}}$	14.57 ± 0.18
$\varepsilon_{\mathrm{cut}} \times \varepsilon_{\mathrm{L0}} \times \varepsilon_{\mathrm{gen}} \times \varepsilon_{\mathrm{rec}}$	0.57 ± 0.01

Table 1 Summary of selection cuts for $\mathrm{B_s^0} \to \mathrm{J/\psi(ee)\phi}$ signal events. Each efficiency is evaluated with respect to previous cut.

3.5 Efficiencies and rates

Tables 3.5 and 3 show the expected number of events for signal and background, and the expected minimum bias rates, respectively.

We can infer from these number that the expected background over signal ratios are we can infer $\frac{B_{\mathrm{b\bar{b}}}}{S} \sim 23$ and $\frac{B_{\mathrm{J/\psi}}}{S} \sim 0.7$. This is based on the cross sections used in DC06 simulation ($\sigma_{bb} = 698 \mu b$

Sample	# events accepted	expected with $2fb^{-1}$
$\mathrm{B_s^0} \to \mathrm{J}/\psi(\mathrm{ee})\phi$ /(with HLT1)	7.8k/(3.9k)	34k/(17k)
Stripped inclusive $b\bar{b}$ /(with HLT1)	11/(7)	788.9k/(502.0k)
inclusive $X \to J/\psi \to e^+e^-$ /(with HLT1)	19/(2)	117.1k/(<23.4k)

Table 2 Numbers of L0-triggered and selected events and the corresponding expectations for $L_{int} = 2fb^{-1}$, falling in the $\mathrm{B_s^0}$ pseudo mass window $[5.2, 5.5]$ MeV/c^2. The numbers obtained with HLT1 trigger are put between brackets. The expectations are derived assuming $\sigma_{bb} = 500\mu b$ and $\sigma(prompt\ \mathrm{J}/\psi) = 1000\mu b$.

B_s **pseudo mass window**	# events accepted	expected rate (Hz)
$[4.6, 6.2]$ GeV/c^2 /(with HLT1)	33/(2)	26.1/(1.6)
$[5.2, 5.5]$ GeV/c^2 /(with HLT1)	6/(0)	4.7(0)

Table 3 Numbers of accepted events and expected rates for the L0-stripped minimum bias sample.

and $\sigma(prompt\ \mathrm{J}/\psi) = 266\mu b$) which give different expectations from the ones shown in table . In particular, the expected number of signal events, including HLT1, rises to 23.7 k events.

3.6 Resolutions and acceptances

3.6.1 Proper time

A fit to the $\Delta t = t^{\mathrm{rec}} - t^{\mathrm{true}}$ distribution, Figure 12 (left), where t^{true} is the true proper time, allows us to estimate the proper time resolution. The weighted average standard deviation of the fit is $\sigma_t \sim 75$ fs. The per-event proper time error distribution is shown in Figure 12 (right): the most probable value is ~ 32 ps showing that the per-event errors are underestimated, which is further confirmed in the pull distribution, Figure 13, for which the average width is 1.78.

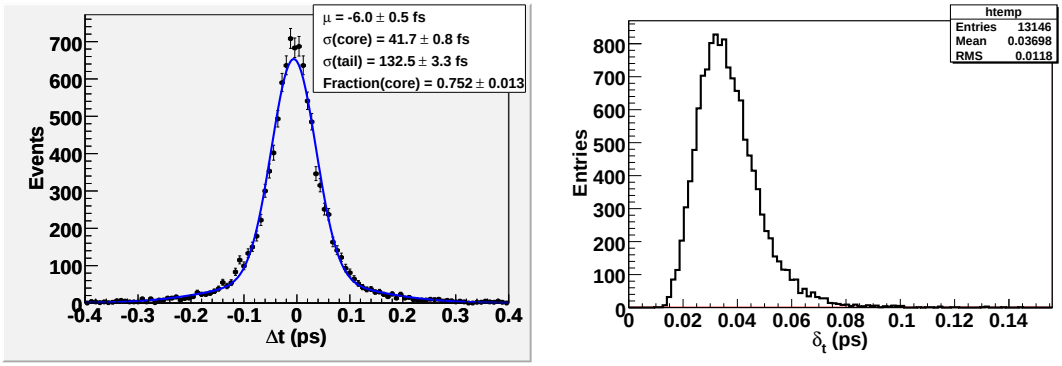

Figure 12 Proper time resolution (left) and per-event fit error (right) distributions for $\mathrm{B_s^0} \to \mathrm{J}/\psi(\mathrm{ee})\phi$.

Figure 14 depicts the proper time acceptance profile for signal events after selection and L0-trigger. We can observe a drop in the first two bins, due to the IPS cut for electrons. The loss of acceptance for higher proper times, $\tau > 6\ ps$ is related to the IP χ^2 ($\mathrm{B_s^0}$) cut.

3.6.2 Transversity angles

Figure 15 shows the (reconstructed - true) residual distributions for the three angles [4]. The weighted average resolution extracted from the fits is 70, 113 and 35 mrad for θ, φ and ψ, respectively. Compared to the $\mathrm{B_s^0} \to \mathrm{J}/\psi(\mu\mu)\phi(\mathrm{KK})$ case, the degradation of resolution is particularly felt for θ and φ as electrons four momenta intervene directly in their calculation. Figure 16 depicts the acceptance profiles for ϕ, $cos(\theta)$ and $cos(\psi)$ for signal events after L0 trigger and selection cuts.

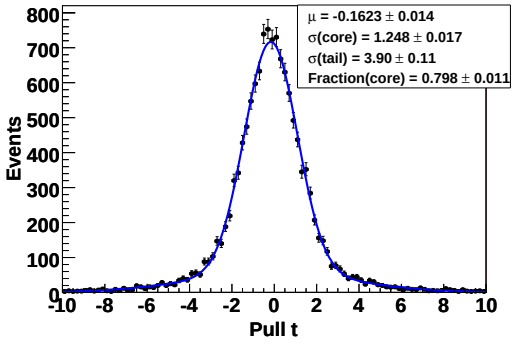

Figure 13 Proper time pull resolution distribution for $\mathrm{B_s^0} \to \mathrm{J}/\psi(\mathrm{ee})\phi$.

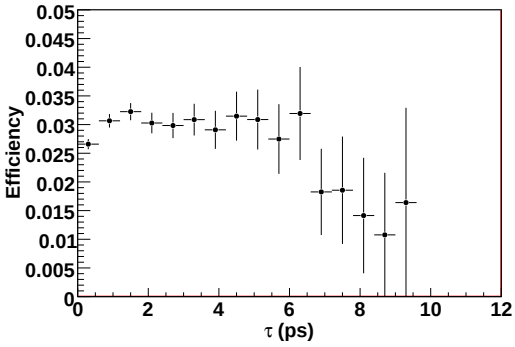

Figure 14 Proper time acceptance for $\mathrm{B_s^0} \to \mathrm{J}/\psi(\mathrm{ee})\phi$.

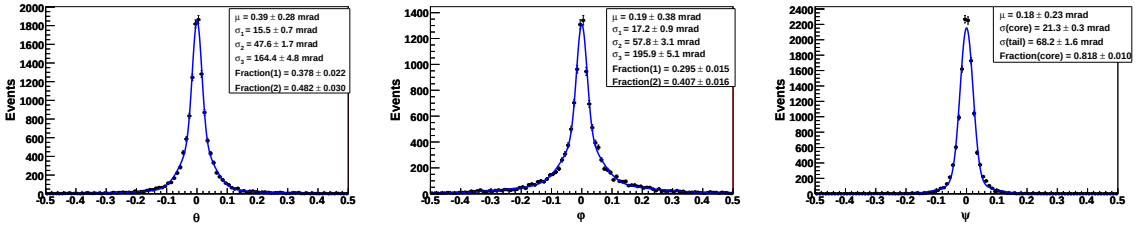

Figure 15 Transversity angles resolution distributions for $\mathrm{B_s^0} \to \mathrm{J}/\psi(\mathrm{ee})\phi$.

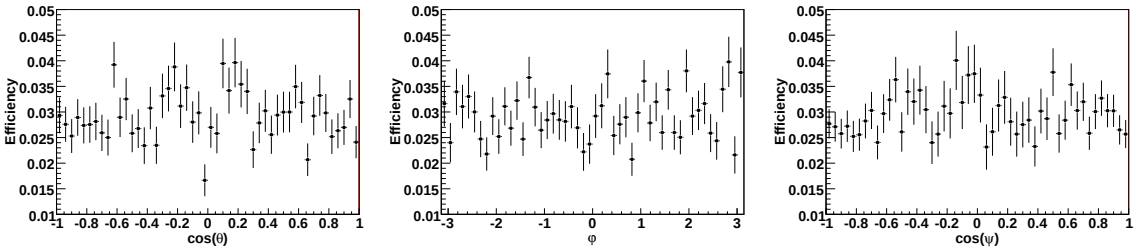

Figure 16 Acceptances of the transversity angles for $\mathrm{B_s^0} \to \mathrm{J}/\psi(\mathrm{ee})\phi$.

4 High Level Trigger selection

Following the same procedure as the offline selection, a study of the selection at the online level has been performed.

4.1 Tracks

The tracks used in the online environment are forward tracks and no particle identification is applied in the current format (apart from electrons or muons).

4.2 Intermediate resonances

4.2.1 $\phi \to \mathrm{K^+K^-}$

For this decay, the distributions do not change much and thus, the cuts are the same as in offline.

4.2.2 $\mathrm{J/\psi \to e^+e^-}$

As for the offline selection electron minimum impact parameter significance is required to be at least 1. For this decay, there is a particular degradation of the reconstruction of the electron energy, and thus the invariant mass of the pair, when using online tracks (see figure 17). The e^+e^- vertex χ^2 per degree of freedom is required to be less than 20 and the invariant mass of the pair must lie within the window $[1500, 3500]$ MeV/c^2 (default base cut) or $[2500, 3500]$ MeV/c^2 (tightened version).

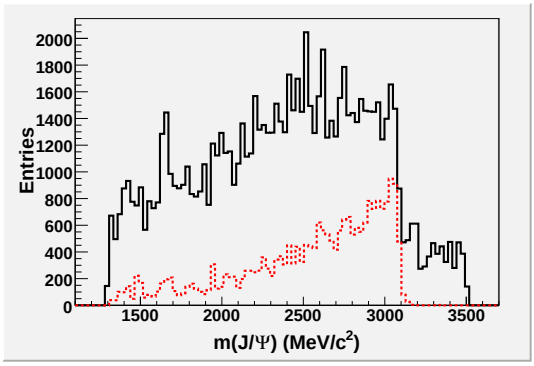

Figure 17 ee invariant mass distribution for all ee pairs (solid black line) and true $\mathrm{J/\psi}$ (red dashed line).

4.3 $\mathrm{B_s^0}$ candidates

To account for the difference with offline environment, the selection cuts are slightly modified as follow:

- the cosine of the angle between the flight vector and the momentum (figure 18), $cos(\vec{F}, \vec{p}) > 0.85$.
- the $\mathrm{B_s^0}$ impact parameter χ^2 (figure 19), $\chi^2_{IP}(\mathrm{B_s^0}) < 400$.
- the $\mathrm{B_s^0}$ vertex χ^2 per degree of freedom (figure 20), $\chi^2_{vtx}/NDoF < 60$.

The final cut is applied on the mass difference $\Delta m = m(\mathrm{B_s^0}) - m(\mathrm{J/\psi})$ (figure 21)
We first start with a loose pre-cut, $1400 < \Delta m < 3100$ MeV/c^2 and then move to a tighter mass window, to reduce the minimum bias events rate.

4.4 Efficiencies and rates

The efficiency is evaluated with respect to events that already passed the offline cuts. With the standard set of cuts consisting of all the cuts described in the previous paragraphs with mass windows $1400 < \Delta m < 3100$ MeV/c^2 and $2500 < m(ee) < 3500$ MeV/c^2, we end up with an efficiency of 75%, which makes the number of expected signal events for a luminosity of 2 fb^{-1} diminishing to 17.8 k events. The corresponding minimum bias rate is 1.5 MHz (198 Hz with HLT1 requirement), which is far too much. As a consequence, tightening some cuts has been considered. Table 4 shows the different attempts.

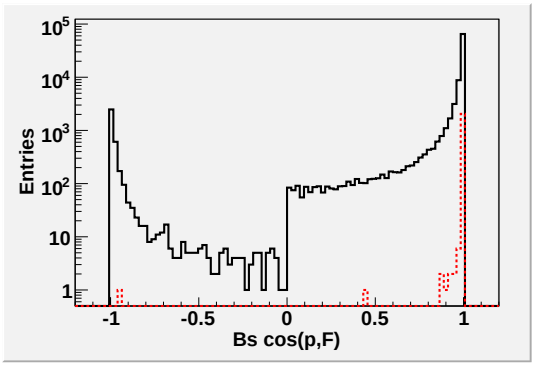

Figure 18 Cosine of the angle between the $\mathrm{B_s^0}$ flight vector and its momentum, for all candidates (solid black line) and true signal (red dashed line).

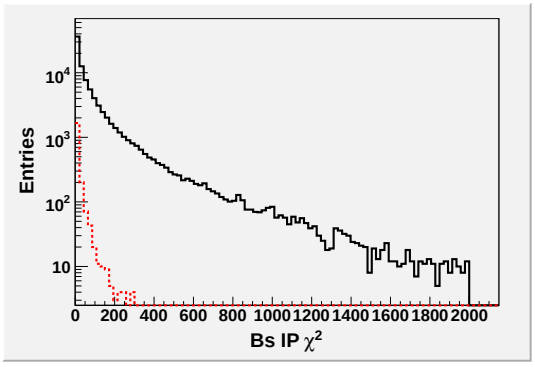

Figure 19 $\mathrm{B_s^0}$ IP χ^2 distribution for all candidates (solid black line) and true signal (red dashed line).

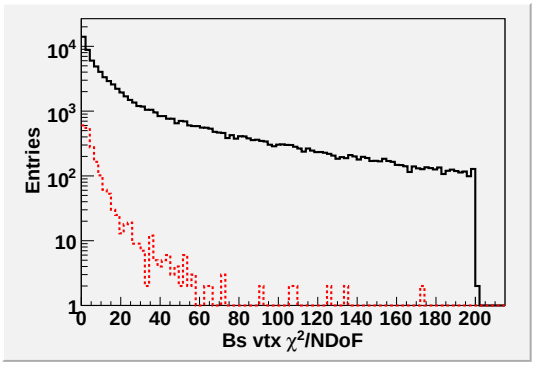

Figure 20 $\mathrm{B_s^0}$ vertex χ^2 per degree of freedom, distribution for all candidates (solid black line) and true signal (red dashed line).

Selection	expected rate (Hz) (with HLT1)
Standard	1500 (198)
+ min IPS(e)>2	328 (47)
+ $1800 < \Delta m < 2500$ MeV/c^2	156 (26)

Table 4 Minimum bias events HLT2 rates for different cut scenarios.

5 Conclusion and outlook

We presented a first complete round for the selection of the channel $\mathrm{B_s^0} \to \mathrm{J}/\psi(\mathrm{ee})\phi$. We found that we can in principle end up with a statistics representing ∼15% of that of $\mathrm{B_s^0} \to \mathrm{J}/\psi(\mu\mu)\phi(\mathrm{KK})$, but with bigger background to signal ratios. If the offline selection minimum bias rate is still accept-

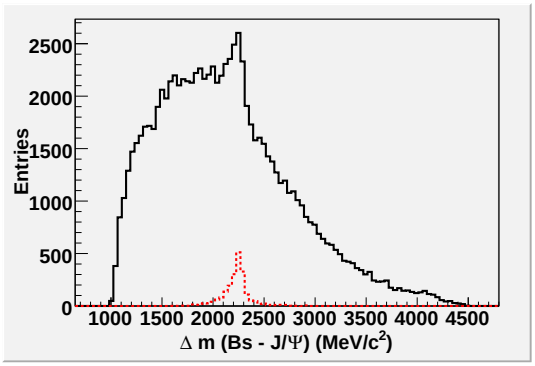

Figure 21 Mass difference $m(\mathrm{B_s^0}) - m(\mathrm{J/\psi})$, distribution for all candidates (solid black line) and true signal (red dashed line).

able, the high level trigger selection leads to big rates[a]. These are engendered by a worsen electron bremsstrahlung reconstruction in the online environment (with DaVinci version v21r0). We will show in a coming documentation that improvements in the online reconstruction can lead to much lower rates and enable retuning of the selections.

6 References

[1] M.Calvi *et al.*, CERN-LHCb-2009-025.

[2] CERN-THESIS-2006-045, CERN-THESIS-2007-051, CERN-THESIS-2007-027.

[3] CERN-THESIS-2005-031

[4] A.Dighe *et al.*, arXiv:hep-ph/951136v1.

[a] These rates are even increased in the subsequent versions of the software, due to improvements in the electron alley.